



Habituated *Moringa oleifera* callus retains metabolic responsiveness to external plant growth regulators

Claude Y. Hamany Djande¹ · Paul A. Steenkamp¹ · Lizelle A. Piater¹ · Ntakadzeni E. Madala¹ · Ian A. Dubery¹

Received: 26 July 2018 / Accepted: 28 January 2019 / Published online: 5 February 2019
© Springer Nature B.V. 2019

Abstract

Undifferentiated plant cells in culture represent a renewable system conducive to understanding biological processes and a valuable alternative for secondary metabolite production. Additionally, manipulation of these systems by plant growth regulators (PGRs) may result in redifferentiation/organogenesis and hence changes in metabolic profiles. The aim of the study was to investigate the effects of combining auxin (2,4-dichlorophenoxyacetic acid) and cytokinin (kinetin) at concentrations of 2, 4, 6 and 9 μM on undifferentiated *Moringa oleifera* callus cells, at a metabolome level. Results indicated that the callus became habituated, i.e. developed the ability to grow without added stimulatory PGRs, and no organogenesis was observed on any of the different PGR combinations under investigation. Methanolic extracts were screened for total phenolic content (TPC) and anti-oxidant activity, and further analysed using liquid chromatography coupled to mass spectrometry combined with multivariate data analysis to facilitate analysis of the metabolite profiles. While the anti-oxidant capacity of extracts from the various treatments exhibited little variation, the TPC differed significantly. Despite the observed habituation phenomenon, the calli retained responsiveness towards external PGRs and each of the 25 conditions generated a unique metabolome as found by principal component analysis. This was also reflected by a number of phytochemicals that were annotated as biomarkers from PGR-treated calli. These findings demonstrate the differential influence of 2,4-D and kinetin on *M. oleifera* callus for the production of secondary metabolites.

Key message

Moringa oleifera callus developed the ability to grow without added stimulatory growth regulators, but retained responsiveness towards external growth regulators, resulting in distinct metabolomes.

Keywords Auxin · Cytokinin · Callus · *Moringa oleifera* · Organogenesis · Secondary metabolites

Abbreviations

BPI	Base peak intensity	GAE	Gallic acid equivalents
CGA	Chlorogenic acid	HCA	Hierarchical clustering analysis
DPPH	2,2'-Diphenyl-1-picrylhydrazyl	<i>m/z</i>	Mass to charge ratio
ESI	Electrospray ionisation	MS	Murashige and Skoog medium
F–C	Folin–Ciocalteu reagent	MSI	Metabolomic Standards initiative
		MVDA	Multivariate data analyses
		OPLS-DA	Orthogonal projection to latent structures-discriminant analysis
		PCA	Principal component analysis
		PGRs	Plant growth regulators
		SIMCA	Soft independent modeling of class analogy

Communicated by Nokwanda Pearl Makunga.

Electronic supplementary material The online version of this article (<https://doi.org/10.1007/s11240-019-01565-y>) contains supplementary material, which is available to authorized users.

✉ Ian A. Dubery
idubery@uj.ac.za

¹ Centre for Plant Metabolomic Research, Department of Biochemistry, University of Johannesburg, Auckland Park, Johannesburg 2006, South Africa

Rt	Retention time
UHPLC–qTOF-HDMS	Ultra-high performance liquid chromatography–quadrupole time-of-flight high definition mass spectrometry

Introduction

The demand for nutritional and medicinal plants is increasing with population growth, and intense industrialization and urbanization (Mughal et al. 1999). As such, cell—and tissue culture may be a very promising technique for in vitro multiplication and conservation of in plant biotechnology (Shahzad et al. 2014). Totipotency is a reflection of the genetic potential of plant cells to produce all of the differentiated cells in the entire plant (Lambé et al. 1997; Ochoa-Villarreal et al. 2015). Isolated cells from differentiated tissue are generally non-dividing and quiescent; to express totipotency they have to undergo dedifferentiation and then redifferentiation. Many plants have been regenerated from single cells, but not all plant cells are totipotent; some are terminally differentiated (Lambé et al. 1997). Plant tissue culture possesses the ability to regenerate organs and even the normal adult plant from a single or group of highly specialised cells, and constitutes an important experimental system for studying cell function and differentiation processes (Loyola-Vargas and Ochoa-Alejo 2012).

In response to endogenous and exogenous stimuli, in vitro regeneration of plants may proceed through direct or indirect organogenesis, with the latter requiring that callus first be produced from the ex-plant. Callus, undifferentiated tissue grown on solid media with the right balance of plant growth regulators (PGRs), is thus the fundamental starting material in most in vitro cultures. Calli can exhibit varying levels of differentiation following the application of PGRs (Radić et al. 2016) such as auxins and cytokinins, the most employed for in vitro cultures (George et al. 2008; Moubayidin et al. 2009; Leljok-Levanić et al. 2016). Differential PGR levels in tissue cultures can be used to manipulate the pattern of regeneration (Loyola-Vargas and Ochoa-Alejo 2012). In general, a higher cytokinin to lower auxin ratio leads to shoot regeneration (caulogenesis), while a low cytokinin to higher auxin ratio leads to root regeneration (rhizogenesis), and the same ratio of both PGRs leads to growth in an unorganized manner (Moubayidin et al. 2009). Interestingly, during long term cultivation, calli from certain plants can lose the requirement for external auxins and cytokinins, and grow in a PGR-independent manner (i.e. exhibit hormonal autonomy), a phenomenon known as habituation (Lambé et al. 1997; Gaspar et al. 2000; Loyola-Vargas and Ochoa-Alejo 2012).

The induction of plant cell—and tissue cultures by external PGR signals may result in the activation of a specific developmental pathway and lead to the regeneration of competent cells (Srisikandarajah et al. 2006). The totipotent characteristic of plant cells in culture makes it a system of choice for secondary metabolite production as a single cell line is able to produce the same range of phytochemicals found in the whole plant under appropriate regimes. Frequently, plant in vitro culture allows the production of secondary metabolites through elicitation and thus the understanding of biochemical processes (Srivastava 2017). Moreover, the controllable environment of in vitro cultures ensures more effective synthesis of targeted compounds (Hellwig et al. 2004; Ochoa-Villarreal et al. 2015, 2016).

Moringa oleifera is a dicotyledonous tree, native to India but also cultivated in some parts of Africa (Saini et al. 2016). The edible leaves of *M. oleifera* possess large amounts of phytochemicals which confer various nutritional, health beneficial and medicinal properties (Gupta et al. 2018; Tiloke et al. 2018), generating an increasing demand for its nutritional and medicinal properties. With *M. oleifera*, the focus of tissue culture is generally to perform in vitro clonal multiplication from nodal and shoot tip explants, as well as for the induction of callus, somatic embryos and morphogenesis (Shank et al. 2013; Shahzad et al. 2014; Salem 2016; Avila-Treviño et al. 2017). However, under in vitro conditions, cultured plant tissue faces an artificial environment leading to possible somoclonal variation and growth aberrations such as vitrification and genetic instability (Kaeppeler et al. 2000). This is also applicable to *M. oleifera* (Hassanein et al. 2018).

In contrast to the in vitro multiplication applications, in this study we investigated the effects of auxin (2,4-dichlorophenoxyacetic acid, 2,4-D) and cytokinin (kinetin, Kin) concentrations on dedifferentiated *M. oleifera* callus cells in an attempt to induce biological variation such as organogenesis that can be linked to differential synthesis of secondary metabolites. In order to screen and study the metabolite profiles resulting from this manipulation, metabolomics tools and approaches were applied.

Materials and methods

In vitro plantlet culture and callus initiation

Seeds were collected from *M. oleifera* trees cultivated in the Limpopo province of South Africa. The surface of the dehusked seeds was decontaminated in a laminar airflow cabinet with 70% (v/v) ethanol for 10 s, then 1.5% (v/v) sodium hypochlorite solution for 20 min and rinsed three times with distilled water (dH₂O). Following decontamination, seeds were germinated in Magenta jars containing 50 mL of basal Murashige and Skoog (MS) medium (Murashige and Skoog

1962) (Duchefa, Haarlem, the Netherlands) solidified with 0.8% agargel™ (Sigma, St Louis, MO, USA) (Fig. S1a).

Callus initiation was carried out in Petri dishes containing MS medium (Murashige and Skoog 1962) enriched with MS vitamins (riboflavin, nicotinic acid, thiamine, and glycine) (Highveld Biologicals, Johannesburg, South Africa). In addition, the medium contained callus-inducing PGRs: 2.2 μM 2,4-D, 21.4 μM alpha naphthalene acetic acid (NAA) (Sigma, St Louis, MO, USA) and 2.3 μM Kin (Duchefa, Haarlem, the Netherlands) (Shank et al. 2013), 30 g/L sucrose as carbon source and 1 g/L hydrolyzed casein (Sigma, Munich, Germany). Agargel™ (8 g/L, Sigma, Munich, Germany) was used as a gel agent and the pH of the medium adjusted to 5.8. Stem sections of 2 week old in vitro grown plantlets were placed on the medium described above and the plates incubated at 24 °C with a light/dark cycle of 16 h/8 h and illumination at 25 μmol/m²/s (Fig. S1b).

Callus manipulation and experimental design

Initiated calli were sub-cultured and multiplied before the manipulation for organogenesis took place. Concentrations (0, 2, 4, 6 and 9 μM) of auxin (2,4-D) and cytokinin (Kin), alone and in combination (actual concentrations and ratios of the 25 conditions are reported in Table S1) were supplemented to MS medium with MS vitamins, sucrose and casein hydrolysate as described. Three replicates were assigned per treatment and the average mass of callus per plate at the start of the experiments was ~2.6 g (Fig. S2).

Metabolite extraction and sample preparation

Calli from each replicate (average mass of 4.8 g) were transferred into pre-weighed, sterile 50 mL Falcon tubes. A volume of 80% methanol (MeOH, analytical grade, Romil, Cambridge, UK) was added in a 1:1 (v/m) ratio and directly put on ice to quench enzymatic activities. Samples were dispersed for 30 min using an ultrasonic bath, then for 1 min at 25 °C using a probe sonicator (Sonopuls, Bandelin, Berlin, Germany) set at 55% power for 20 s intervals. Homogenized samples were centrifuged at 5100×g for 30 min at 4 °C and the supernatants carefully removed. The hydromethanolic supernatants were concentrated to 2 mL by vacuum evaporation using a rotary evaporator, transferred to Eppendorf tubes and evaporated to dryness in a centrifugal vacuum concentrator (Eppendorf, Hamburg, Germany). Dried extracts were reconstituted in 500 μL of 50% MeOH and stored at –20 °C. For ultra-high performance liquid chromatography—quadrupole time-of-flight mass spectrometry (UHPLC–qTOF-MS) analysis, extracts were filtered through 0.22 μm nylon filters into chromatography vials fitted with inserts and slitted caps.

Total phenolic content (TPC) assay

The TPC was determined by the Folin–Ciocalteu (F–C) assay (Ainsworth and Gillespie 2007) in 2 mL Eppendorf tubes. Briefly, to 100 μL of each extract, blanks (80% MeOH) and a concentration series of gallic acid (Sigma, St Louis, MO, USA) dissolved in 80% MeOH, 200 μL of 10% (v/v) F–C reagent (Sigma, St Louis, MO, USA) was added and vortexed thoroughly. A volume of 800 μL of 0.7 M sodium carbonate (Na₂CO₃) was then added to the mixture and incubated at room temperature for 2 h. After incubation, 200 μL of each test sample, blank and standard (positive control) was transferred in triplicate to a 96-well microplate and the absorbance determined at 765 nm using a microplate reader. Concentrations of gallic acid employed to generate the calibration curve were between 250 μM and 1250 μM. All experiments for TPC were performed in triplicate. The results obtained were statistically expressed as mean ± standard deviation (SD).

Anti-oxidant assay

A volume of 150 μL of a freshly prepared solution of 150 μM 2,2'-diphenyl-1-picrylhydrazyl (DPPH) (Sigma, St Louis, MO, USA) dissolved in 80% MeOH was added to a 96-well plate followed by 50 μL of each extract, blank (80% MeOH) and standard. Each sample was added to the plate in triplicate and solutions were mixed, covered and incubated in the dark for 4 h. The absorbance was then read at 517 nm. Vitamin C was utilized as standard anti-oxidant at concentrations varying from 20 μM to 200 μM (Esterhuizen et al. 2006) to construct the calibration curve. The DPPH radical inhibition activity was calculated according to the equation: % DPPH inhibition = $[(A_{\text{blank}} - A_{\text{sample}})/A_{\text{blank}}] \times 100$. All experiments for anti-oxidant assays were performed in triplicate and the results obtained statistically expressed as mean ± SD.

Ultra-high performance liquid chromatography–quadrupole time-of-flight high definition mass spectrometry (UHPLC–qTOF-HDMS)

Chromatographic analyses of extracts were performed on an Acquity Classic UHPLC system (Waters Corporation, Milford, MA, USA) coupled to a SYNAPT G1 high definition quadrupole time-of-flight (qTOF) mass spectrometer (Waters Corporation, Milford, MA, USA). Separation of extracts was carried out on a Waters Acquity UHPLC column (HSS T3 C18 reverse phase column, 150×2.1 mm with a 1.8 μm particle size). The gradient elution was performed with eluent A (0.1% formic acid in water) and eluent B (0.1% formic acid in acetonitrile) at a flow rate of 0.4 mL/min. The injection volume was 3 μL. The elution

was initiated with 2% of eluent B for 1 min, and was kept constant for 2 min. The gradient was introduced by increasing B to 3%, 8% then 50% for 1, 21 and 1 min respectively. The eluent B concentration was finally increased to 95% for 2 min before restoration to the initial condition (2% B) for 2 min. Each sample was injected in triplicate and analyzed in a randomized order.

The separated compounds were further detected using a SYNAPT G1 qTOF–MS system set in V-optics and operated in negative electrospray ionization (ESI) mode. The analyses were set to perform unfragmented and four fragmenting experiments (MS^E) concurrently by collision energy ramping from 10 to 40 eV. The reference calibrant was leucine enkephalin (9×10^{-17} M, 554.2615 Da) at a flow rate of 0.1 mL/min, and a mass accuracy window of 0.5 mDa was maintained throughout the analysis. The source and desolvation gas temperatures were set at 120 and 450 °C respectively, and the cone gas and desolvation gas flows were at 50 and 550 L/h respectively. The interscan time was 0.02 s, the scan time 0.1 s covering a mass to charge (m/z) range of 100–1000. The capillary voltage was 2.5 kV, the extraction cone voltage 4 V and the sampling cone voltage 30 V.

Data processing and multivariate data analysis

The extracted raw UHPLC–MS data sets were processed for matrix generation using the MarkerLynx XSTM application manager tool of MassLynx XS software, version 4.1 (Waters Corporation, Milford, MA, USA). The MarkerLynx application employed the patented ApexPeakTrack algorithm to achieve accurate peak detection and alignment. A modified Savitzky-Golay smoothing and integration are performed by MarkerLynx software prior the calculation of intensities. Additionally, based on total ion intensities of each distinct peak, MarkerLynx performs sample normalization. The parameters were set to process the retention time (Rt) range 1.5–25.0 min of the chromatogram, mass range 100–1000 Da, mass tolerance 0.01 Da, mass window 0.05 Da and a Rt window of 0.20 min.

The resulting data matrices were exported to ‘soft independent modelling of class analogy’ (SIMCA) software, version 14 (Umetrics Corporation, Umeå, Sweden) for multivariate data analysis. All data were *Pareto*-scaled and mean-centered to put all variable on the same footing, adjust for measurement errors and minimize variable redundancy. In order to simplify and reduce the dimensionality of the datasets, differentiate between treatments and explain the metabolic changes between samples, chemometrics/multivariate data analyses (MVDA) that included principal component analysis (PCA) and hierarchical clustering analysis (HCA), were used (Tugizimana et al. 2013). The orthogonal projection to latent structures-discriminant analysis (OPLS-DA) modelling was used as a supervised method to identify

discriminatory biomarkers by revealing hidden biological differences from metabolite profiles (Tugizimana et al. 2013). Diagnostic tools such as the cumulative model variation in the matrix X, R^2X (*cum*), which is the goodness-of-fit parameter that describes the proportion of the variance of the total variation explained by the model and the predictive ability, Q^2 were employed to evaluate generated models. The analysis of variance testing of cross-validated predictive residuals (CV-ANOVA), another diagnostic tool (with p -value ≤ 0.05 indicating a good model), was employed to statistically assess the reliability of the OPLS-DA models generated. Models were validated using the receiver operator characteristic (ROC) plots. The statistical significance and discriminability of biomarkers selected from the OPLS-DA S-plots (features or variables) were assessed with the variable importance in projection (VIP) plots.

Metabolite annotation and identification

The raw analytical data obtained required conversion to metabolite information in order to assist with the biological interpretation. In this study, annotation of the detected metabolites was based on mass spectral data. Fragmentation patterns provided by the mass spectral data are often compound-specific and can help in the process of identification (Kind and Fiehn 2007). The first step of the compound identification here was the acquisition of accurate mass. This was followed by the calculation of the elemental composition formulae corresponding to the measured accurate mass. Databases such as Dictionary of Natural Products (DNP) (<http://www.dnp.chemnetbase.com>), ChemSpider (<http://www.chemspider.com>) and Knapsack (<http://kanaya.naist.jp/KNAPSAcK/>) were used to search for compounds corresponding to the calculated elemental composition formulae. Metabolites were annotated according to the metabolomic standards initiative (MSI) level-2 (Sumner et al. 2007), using MS fragmentation patterns and data from the literature. The literature available on the MS-based identification of specific compounds was cited to provide additional supportive information. Finally, MetaboAnalyst (statistical, functional and integrative analysis of metabolomics data), <https://www.metaboanalyst.ca/>, was used as a clustering and visualisation tool for heatmap construction.

Results

Moringa oleifera callus development and growth

Moringa oleifera callus manipulated with 2,4-D and Kin at different concentrations and molar ratios (Table S1) showed no organ formation in all treatments after 21 days of incubation (Fig. S2). Callus texture and appearance varied

according to the PGRs ratio, and calli obtained after incubation were mostly friable and beige to yellowish in colour (Fig. S2). The mass of calli collected ranged from 3.08 to 6.03 g with the lowest mass obtained where 9D:0K was added (9 μ M of 2,4-D) (Table 1, Fig. S3). In contrast, the highest mass was obtained with 2D:4K. In the case of Kin alone, the masses tend to increase from 0D:2K (2 μ M) to 0D:6K (6 μ M) and finally decreases with 0D:9K (9 μ M). In contrast, with 2,4-D, there were increases in mass for 2D:0K (2 μ M), 4D:0K (4 μ M), 6D:0K (6 μ M) and a decrease with 9D:0K (9 μ M).

Total phenolics and anti-oxidant content

The concentration of phenolics in each sample was expressed in μ g gallic acid equivalents (GAE)/g wet (undried) weight and is presented in Table 1 and Fig. S3. The highest concentration of phenolics (49.86 μ g GAE/g wet weight) was observed with 6D:4K (6 μ M of 2,4-D and 4 μ M of Kin) suggesting this as the most favourable PGR combination for phenolic compound production by *M. oleifera* callus. An increase in the content of phenolic compounds was observed where only 2 μ M of 2,4-D was employed (2D:0K), followed by a decrease with 4D:0K, 6D:0K and 9D:0K (highlighted in light grey). In the case of Kin applied alone, the concentration of phenolic compounds decreased in comparison to the control (highlighted in mid grey). This indicates that Kin alone does not induce the production of phenolic compounds in *M. oleifera* callus. A positive correlation was observed between the phenolic content in *M. oleifera* callus and the addition of equal concentrations of both 2,4-D and Kin (2D:2K, 4D:4K, 6D:6K, indicated in dark grey) but the

TPC finally decreased where concentrations of both PGRs reached the highest values (9D:9K).

In contrast to the TPC determinations, the anti-oxidant activity determination showed little variation between the 25 conditions, with the % inhibitory activity varying between 61% (0D:9K; 0 M of 2,4-D and 9 μ M of Kin) and 78% (4D:2K; 4 μ M of 2,4-D and 2 μ M of Kin) (results not shown).

UHPLC–MS and MVDA

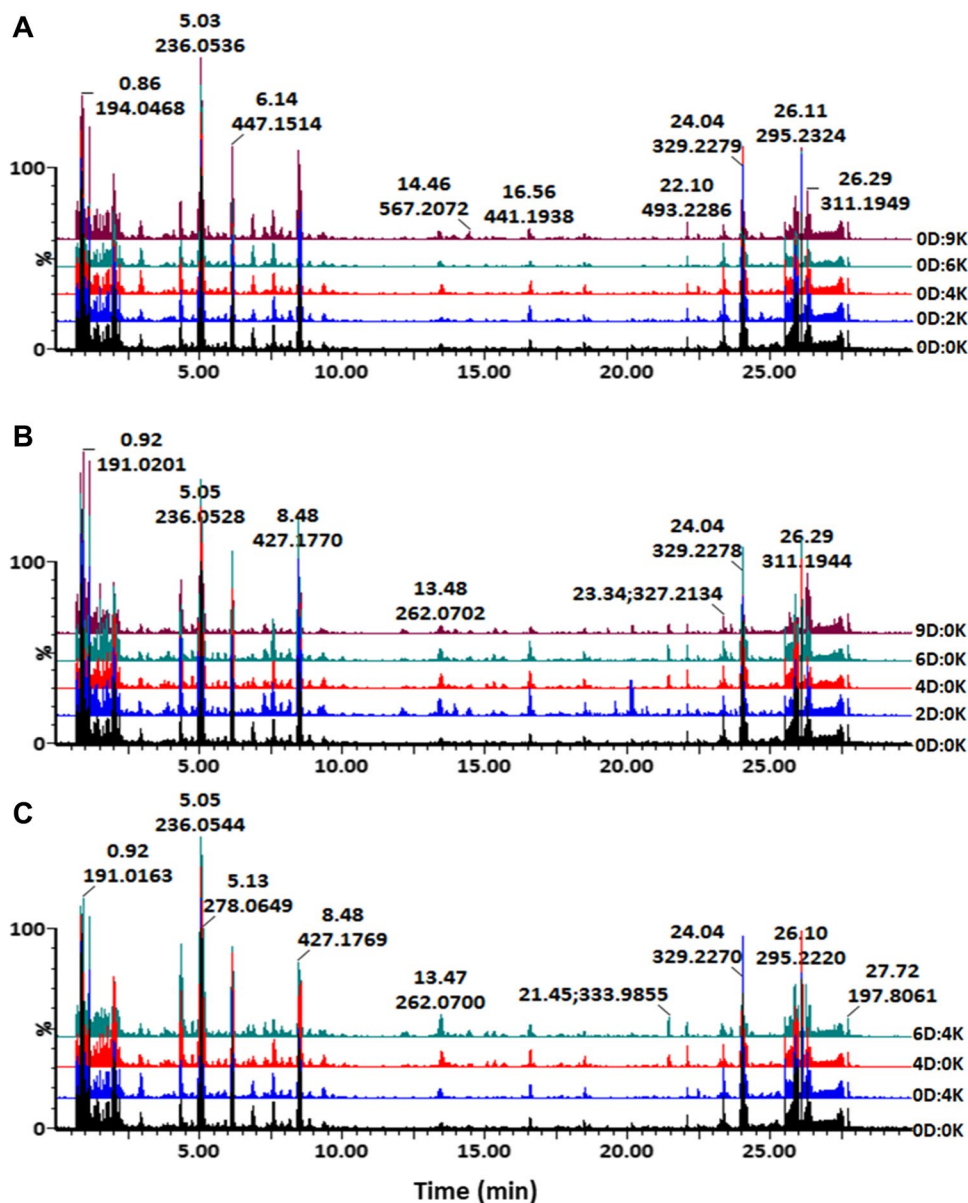
The methanolic extracts were analyzed by UHPLC–qTOF–MS to investigate the metabolite variation following growth of callus on different concentrations and molar ratios of 2,4-D and Kin. UHPLC–MS base peak intensity (BPI) chromatograms obtained in negative ESI mode are presented in Fig. 1. The comparison of MS chromatograms showing samples treated with Kin alone (Fig. 1a) displays a very slight or no difference in peak intensity. In the case of 2,4-D (Fig. 1b), there are differences mostly in terms of peak intensity but also with regard to the presence/absence of some peaks. Figure 1c was constructed as a summary showing overlaid chromatograms comparing the control (0D:0K), Kin (represented by 0D:4K), 2,4-D (represented by 4D:0K) and a combination of both Kin and 2,4-D (represented by 6D:4K). Here, one condition was chosen per group (Kin, 2,4-D and combinations) to simplify the observations. Overall, differential effects of the PGR composition of the medium (especially in the presence of 2,4-D alone or in combination with Kin) on the secondary metabolite profiles of *M. oleifera* callus were observed. It is noteworthy to mention that the most intense peaks appear to be in the early Rt regions of the chromatograms, indicating the relative hydrophilicity of metabolites

Table 1 Template of *M. oleifera* callus cultivated on 25 different molar concentrations and ratios of 2,4-D and Kinetin, with the corresponding total phenolic content (μ g GAE/g wet weight)

PGR	Auxin (2,4-D)					
	Conc. (μ M)	0	2	4	6	9
Cytokinin (Kinetin)	0	0D:0K 33.66 \pm 0.02	2D:0K \uparrow 36.55 \pm 0.02	4D:0K \downarrow 30.93 \pm 0.04	6D:0K \downarrow 29.31 \pm 0.03	9D:0K \downarrow 29.39 \pm 0.01
	2	0D:2K \downarrow 28.05 \pm 0.05	2D:2K \uparrow 35.56 \pm 0.01	4D:2K 34.83 \pm 0.01	6D:2K 26.73 \pm 0.01	9D:2K 35.18 \pm 0.01
	4	0D:4K \downarrow 23.56 \pm 0.02	2D:4K 31.99 \pm 0.02	4D:4K \uparrow 34.55 \pm 0.02	6D:4K 49.86 \pm 0.03	9D:4K 32.78 \pm 0.05
	6	0D:6K \downarrow 30.30 \pm 0.03	2D:6K 32.57 \pm 0.01	4D:6K 36.41 \pm 0.01	6D:6K \uparrow 39.65 \pm 0.02	9D:6K 32.25 \pm 0.03
	9	0D:9K \downarrow 32.37 \pm 0.02	2D:9K 31.47 \pm 0.02	4D:9K 31.89 \pm 0.01	6D:9K 35.05 \pm 0.03	9D:9K \downarrow 31.70 \pm 0.03

The control is condition 0D:0K (habituated state, no added hormones); light grey concentrations in callus grown on 2,4-D alone; mid grey represents concentrations in callus grown on kinetin alone and dark grey represents equal concentrations of kinetin and 2,4-D. The highest concentration of phenolics was found at the 6D:4K ratio. The arrows indicate the increase or decrease in phenolic content compared to the control

Fig. 1 UHPLC–MS (ESI negative mode) BPI chromatograms of methanol extracts from *M. oleifera* callus. **a** Chromatograms of callus treated with Kin only, **b** Chromatograms of callus treated with 2,4-D only, and **c** Chromatograms comparing callus treated with Kin alone, 2,4-D alone and a combination of both (as indicated) in comparison to no PGRs



in that region. In order to reveal clearer differences in the metabolite profiles of *M. oleifera* callus treated with different concentrations of PGRs, MVDA were performed.

MVDA are employed to extract significant information from large and complex sets of data resulting from metabolomic studies. MVDA includes two groups of analyses: unsupervised approaches such as PCA and HCA; and supervised approaches such as OPLS-DA (Tugizimana et al. 2013). As seen in Fig. 2 representing the PCA score plots (Fig. 2a, b) and the HCA plots (Fig. 2c, d) of *M. oleifera* callus extracts, samples are differentially clustered according to the PGR treatment. Kin-treated samples are seen to group close to the control and a clear difference is observed with 2,4-D treated samples, clustering separately from the control. This highlights the differential effect of the 2,4-D in

the production of secondary metabolites. Moreover, extracts containing the combination of Kin and 2,4-D are grouped together with 2,4-D employed alone; an indication that this PGR is primarily responsible for the variation between the samples.

Further descriptive exploration of data was performed using OPLS-DA, and biomarkers corresponding to each condition were extracted. Due to the number of conditions, only examples of an OPLS-DA model are shown here (Figs. S4a, c: control vs. Kin treatments, and Figs. S5a, c: control vs. 2,4-D treatments). All conditions displayed a similar trend whereby the control was separated from all the treatments. Models were further validated using ROC plots (Figs. S4b, S5b) summarizing the performance of the OPLS-DA. The statistical significance and discriminability

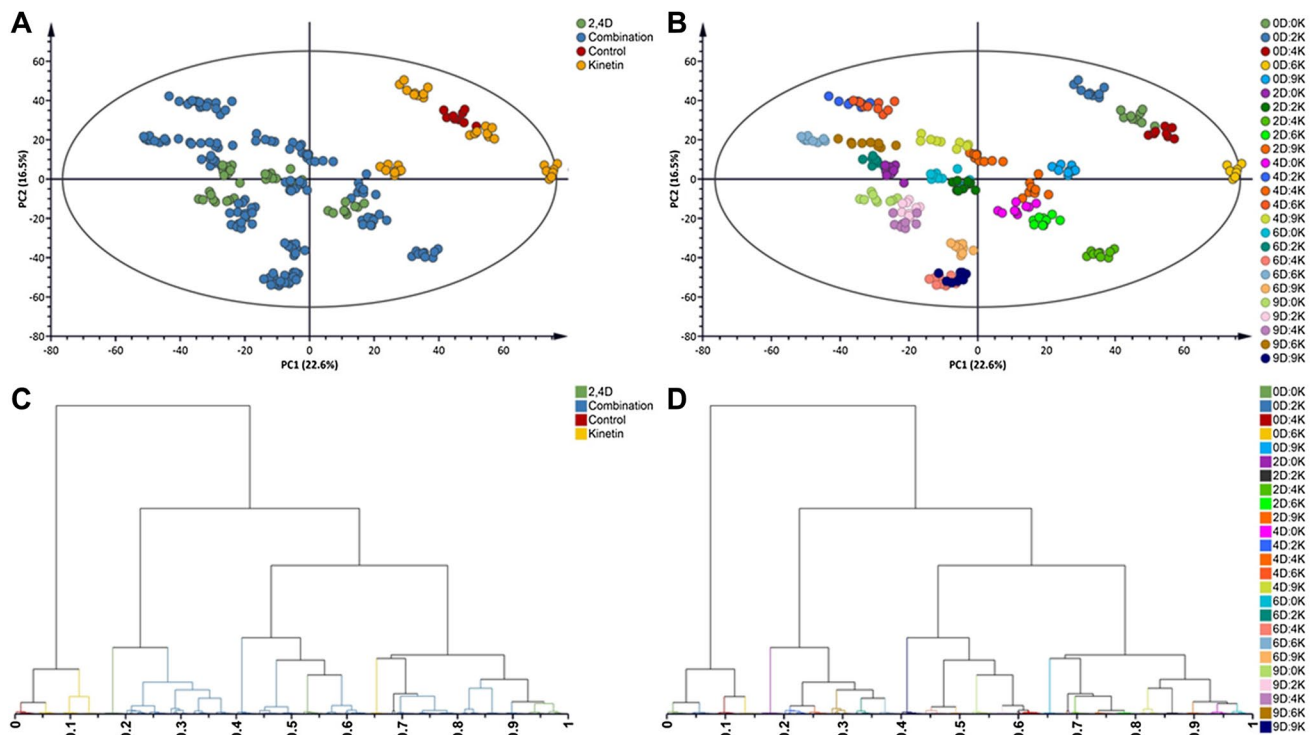


Fig. 2 Unsupervised multivariate data modelling methods. **a, b** Principal component analyses (PCA) showing the different grouping and separation of *M. oleifera* samples treated with different concentrations and ratio of PGRs (Table 1) and analyzed by UHPLC–MS in ESI neg mode. The score plot generated was coloured accord-

ing to the group (a) and according to each treatment (b). The model calculated 17 components and yielded $R^2X_{(cum)} = 73.4\%$ and $Q_{(cum)} = 57.2\%$. **c, d** HCA dendrograms applied on PCA (a) and (b) respectively

of biomarkers selected from the S-plots (features or variables) were also assessed with VIP plots (Figs. S4d, S5d). The selected features with VIP scores > 1.0 were considered as significant in contributing to the class separation (Tugizimana et al. 2016). The selected features were, therefore, considered as important phytochemicals explaining the metabolic changes occurring in *M. oleifera* callus grown in the presence of different ratios of 2,4-D and Kin.

Metabolite annotation

The identification of metabolites can be putative (using accurate mass and mass spectral fragmentation patterns) or definitive (using more than two molecular properties, authentic standard and in vivo labeling methods for confirmation) Following differential treatment with 2,4-D and Kin, untargeted metabolite profiling of the *M. oleifera* callus revealed specific classes of secondary metabolites (derivatives of hydroxybenzoic acids and hydroxycinnamic acids) and primary metabolites (organic acids, amino acids, and fatty acids) (Table 2).

Secondary metabolites: phenolic compounds and derivatives

A total of eight phenolic compounds (two quinic acid isomers, four hydroxycinnamic acid derivatives, one hydroxybenzoic acid and a benzoic acid intermediate) were annotated. These were identified as biomarkers, associated with the different treatments as indicated in Table 2.

Two compounds corresponding to quinic acid stereoisomers (precursor ion at m/z 191) eluted at $R_t = 0.92$ and 1.12 min, giving fragments of m/z 173 corresponding to the mass of a dehydrated quinic acid and m/z 111 resulting from a decarboxylation and two dehydration events of quinic acid (Deshpande et al. 2016). The compounds were not identified as statistically significant biomarkers but were detected in all conditions. Quinic acid has eight stereoisomers which can occur naturally in plants (Deshpande et al. 2016).

A molecule with a precursor ion of m/z 341 [(M–H)[–], $R_t = 4.79$ min] exhibited MS fragment ions of m/z 179 corresponding to the caffeic acid resulting from the loss of a hexose moiety, and 135 corresponding to a decarboxylated caffeic acid. The compound was putatively annotated as caffeoyl hexose based on the fragmentation pattern. The

Table 2 Signatory biomarker-metabolites annotated from methanolic extracts of *M. oleifera* callus cultivated on different concentrations and molar ratios of 2,4-D and kinetin alone, and in combination

	Name	Empirical formula	R _t	MW	Precursor ion <i>m/z</i>	MS fragments	Conditions ^a
	Quinic acid isomer I	C ₆ H ₈ O ₇	0.92	192	191.016	173, 111	#
	Quinic acid isomer II	C ₆ H ₈ O ₇	1.12	192	191.016	173, 111	#
A	Caffeoyl hexose	C ₁₅ H ₁₈ O ₉	4.79	342	341.086	179, 135	0D:9K, 2D:0K, 2D:2K, 2D:4K, 2D:6K, 2D:9K, 4D:0K, 4D:6K, 4D:9K, 6D:0K, 6D:2K, 6D:4K, 6D:6K, 6D:9K, 9D:0K, 6D:2K
B	Caffeoyl dihexose	C ₂₁ H ₂₈ O ₁₄	3.76	504	503.139	341, 179, 135	2D:6K, 2D:9K, 4D:0K, 6D:4K, 6D:6K, 6D:9K, 9D:0K, 9D:2K, 9D:4K, 9D:6K, 9D:9K
C	Coumaroyl aspartate/hydroxy-cinnamoyl aspartate	C ₁₃ H ₁₃ NO ₆	4.32	279	278.063	163, 132	0D:2K, 0D:4K, 0D:6K, 0D:9K, 2D:0K, 2D:2K, 2D:4K, 2D:6K, 2D:9K, 4D:0K, 4D:2K, 4D:4K, 4D:6K, 4D:9K, 6D:0K, 6D:2K, 6D:4K, 6D:6K, 6D:9K, 9D:0K, 9D:2K, 9D:4K, 9D:6K, 9D:9K
D	Coumaroyl hexose	C ₁₅ H ₁₈ O ₈	4.88	326	325.091	163, 119	0D:9K, 2D:0K, 2D:9K, 4D:2K, 6D:2K, 6D:4K, 6D:6K, 6D:9K, 9D:0K, 9D:2K, 9D:4K, 9D:6K, 9D:9K
E	Protocatechuic acid hexose/3,4 dihydroxy benzoic acid	C ₁₃ H ₁₆ O ₉	1.99	316	315.067	152, 153	0D:6K, 2D:4K, 2D:6K, 2D:9K, 4D:0K
	Benzylalcohol-hexose-pentose isomer I	C ₁₈ H ₂₆ O ₁₀	5.66	402	401.147	269, 161, 101	#
F	Benzylalcohol-hexose-pentose isomer II	C ₁₈ H ₂₆ O ₁₀	5.92	402	401.140	269, 161, 101	0D:0K
G	Benzylalcohol-hexose-pentose isomer III	C ₁₈ H ₂₆ O ₁₀	6.13	402	447.144	269, 161, 101	0D:0K
H	Phenylalanine	C ₉ H ₁₁ NO ₂	1.80	165	164.069	147	0D:2K, 0D:4K
I	Tryptophan	C ₁₁ H ₁₂ N ₂ O ₂	2.91	204	203.080	159/158, 142, 116	0D:4K, 0D:6K, 0D:9K, 9D:9K
J	Tryptophan conjugate	–	2.88	275	274.091	159/158, 142, 116	0D:4K, 0D:6K, 0D:9K, 2D:0K, 2D:2K, 2D:4K, 2D:6K, 2D:9K, 4D:0K, 4D:4K, 6D:4K, 6D:9K, 9D:4K, 9D:9K
K	Butanyol hexose pentose	C ₁₅ H ₂₆ O ₁₁	8.51	382	381.171	249, 160/161, 101/100	0D:2K, 0D:9K, 2D:0K, 2D:2K, 4D:2K, 4D:6K, 4D:9K, 6D:2K, 6D:6K, 9D:0K, 9D:2K, 9D:6K

Table 2 (continued)

	Name	Empirical formula	R _t	MW	Precursor ion <i>m/z</i>	MS fragments	Conditions ^a
	Trihydroxyoctadecadienoic acid isomer I	C ₁₈ H ₃₂ O ₅	23.24	328	327.212	171	#
L	Trihydroxyoctadecadienoic acid isomer II	C ₁₈ H ₃₂ O ₅	23.34	328	327.215	229, 211, 171	0D:4K, 0D:6K
	Trihydroxyoctadecenoic acid isomer I	C ₁₈ H ₃₄ O ₅	23.43	330	329.230	211, 171	#
	Trihydroxyoctadecadienoic acid isomer III	C ₁₈ H ₃₂ O ₅	23.48	328	327.219	171	#
M	Trihydroxyoctadecenoic acid isomer II	C ₁₈ H ₃₄ O ₅	24.03	330	329.234	211, 171	0D:4K, 0D:6K
N	Trihydroxyoctadecadienoic acid isomer IV	C ₁₈ H ₃₂ O ₅	24.7	328	327.215	171	0D:2K

Biomarkers were annotated as described under Experimental and in the text

^aConditions (micromolar ratios) in which compounds were found as biomarkers (numbered according to Table S1)

[#]Compounds identified during profiling (not selected as biomarkers)

molecule was present as biomarker mostly in samples treated with 2,4-D alone (2D:0K, 4D:0K, 6D:0K, 9D:0K) and conditions containing a mixture of both 2,4-D and Kin. A similar molecule was detected at *R*_t = 3.76 min with *m/z* 503 [M–H][–], displaying fragments of *m/z* 341 for caffeoyl-hexose due to the loss of another molecule of hexose (162), 179 for caffeic acid and 135 for caffeoyl moiety without CO₂. The latter was characterized as caffeoyl-dihexose (Ncube et al. 2014; Fusani et al. 2016). The up-regulation of this compound was observed in callus grown on 2,4-D alone and in combination with Kin. A molecule with a precursor ion *m/z* 278 [M–H][–] was detected at *R*_t 4.32 min and produced a fragment ion of *m/z* 163, corresponding to a coumaric acid residue and an intense fragment of *m/z* 132 corresponding to an aspartic acid moiety. The compound was characterized as coumaroyl aspartate (Keller et al. 1996; Pereira-Caro et al. 2013) and was found to be up-regulated in all conditions in comparison to the control. The last hydroxycinnamic acid derivative with a precursor ion at *m/z* 325 was observed at *R*_t 4.88 exhibiting daughter ions of *m/z* 163 (coumaric acid) due to the loss of a sugar moiety and 119 for decarboxylated coumaric acid (Bystrom et al. 2011). Based on the fragmentation pattern, the compound was putatively identified as coumaroyl hexose, and highlighted as a discriminant ion in conditions containing the highest concentration Kin with increasing concentrations of 2,4-D (0D:9D, 2D:9K, 6D:9K and 9D:9K).

With regard to hydroxylated benzoic acid derivatives, a molecule with a precursor ion at *m/z* 315.067 [M–H][–] was detected at *R*_t 1.99 min. The MS fragmentation pattern exhibited ions at *m/z* 153 corresponding to the protocatechuic acid ion resulting from the neutral loss of hexose (162) and *m/z* 109 representing decarboxylated protocatechuic acid. The molecule was tentatively annotated as

protocatechuic acid (3,4 dihydroxybenzoic acid)-hexose (Morreel et al. 2014) and identified as a significant ion in 0D:6K, 2D:4K, 2D:6K, 2D:9K, 4D:0K.

In the same category of compounds, the following molecule with a precursor ion *m/z* 401 [M–H][–] which eluted at the *R*_t = 5.66 min was also characterized. This compound produced daughter ions at *m/z* 269 resulting from a neutral loss of a pentose moiety and *m/z* 161 due to the loss of both pentose and hexose moieties. The compound was annotated as benzyl alcohol hexose-pentose, and its two additional isomers were also identified at *R*_t 5.92 (isomer II) and 6.13 min (isomer III) (Bystrom et al. 2011; Barros et al. 2012; Karar and Kuhnert 2015). Benzyl alcohol hexose-pentose isomers II and III were found to be down-regulated in all conditions as compared to the control. The isomer I (*R*_t = 5.66 min) was not considered as a statistically significant biomarker but was identified in extracts.

Primary metabolites

Two amino acids were identified in *M. oleifera* callus as putative biomarkers. Phenylalanine (Phe) and tryptophan (Trp), with precursor ions of *m/z* 164 and 203 respectively, were characterized as previously described by Rodriguez-Perez et al. (2015) in *M. oleifera* leaves.

In the same group of organic compounds, a disaccharide molecule was annotated based on DNP data and its fragmentation pattern. The molecule produced precursor ion at *m/z* 381 with fragment ions of *m/z* 249 resulting from the loss of a pentose (132), another product ion at *m/z* 161 due to subsequent to the loss of a pentose and two carbons dioxides. Hence, the molecule was putatively annotated as butanoyl hexose pentose and extracted from OPLS-DA as a biomarker for conditions indicated in the Table 2. Lastly,

four isomers of trihydroxyoctadecadienoic acid with precursor ion at m/z 327 were detected at R_t s = 23.24, 23.34, 23.48 and 24.7 min respectively. The fragment ions at m/z 211 and 229 resulting from the cleavage of C_{12} and C_{13} bonds, and a subsequent loss of water were characteristic of these isomers (Rodríguez-Pérez et al. 2015). Similarly to this compound, two isomers of trihydroxyoctadecenoic acid (m/z 329) were also identified with similar fragments at R_t s = 23.43 and 24.03 min.

Occurrence of the metabolites

The occurrence of identified and annotated biomarkers between samples was highlighted using a color-coded heatmap (Fig. 3) showing the occurrence of selected metabolites among the treatments. 2,4-D and Kin treatments resulted in a differential distribution of the identified compounds among samples, depending on the concentrations and molar ratios of the two PGRs. For instance, caffeoyl hexose (A), caffeoyl dihexose (B), coumaroyl aspartate (C) and coumaroyl hexose (D) seem to be absent or present in relatively low concentrations in the presence of Kin alone. At high concentration of 2,4-D with varying concentrations of Kin, these compounds (A, B, C and D) are more prominent. Except for butanoyl hexose pentose (K), all the primary metabolites as well as the secondary metabolites protocatechuic acid hexose (E) and benzyl alcohol hexose-pentose isomer I and II (F and G respectively) are more prominent in presence of Kin alone.

The occurrence of selected biomarkers between samples was highlighted using a color-coded PCAs score plots (Fig. 4). As seen in the figure, coumaroyl aspartate and caffeoyl dihexose (Fig. 4b, c) are more prominent in the extracts from callus grown on 2,4-D and combinations

thereof. By comparison, protocatechuic hexose and benzyl alcohol hexose-pentose (Fig. 4d, e) were more intense in extracts from callus grown where Kin was the dominant PGR.

Discussion

Moringa oleifera callus development and growth

The variation of masses observed shows that concentration and ratio of the two PGRs did affect the growth rate (and thus the responsiveness) of the callus. Callus texture and appearance can vary according to the plant species and more precisely the part of the plant used as ex-plant (Loyola-Vargas and Ochoa-Alejo 2012). The callus of *M. oleifera* initiated from any type of ex-plant has been reported by Shank et al. (2013) to be friable, soft and white to yellowish in colour. The friability of a callus presents the advantage of being appropriate for suspension cultures and favourable for secondary metabolite production (Shank et al. 2013).

It was observed that the callus grew well on PGR-free media, an ability that was retained over several generations of sub-culture. This suggests that *M. oleifera* cells acquired the capability to grow in the absence of the externally added PGRs, a phenomenon known as habituation (Leljak-Levanić et al. 2016). Habituation is a multi-step phenomenon that occurs gradually and may lead to complete and irreversible dedifferentiation of cells (Hagege 1996; Gaspar et al. 2000). Although the causes of habituation are still unclear, it has been proposed that it might be due to the increase in the biosynthesis or the decrease of the degradation rate of endogenous phytohormones, the altered sensitivity of cells

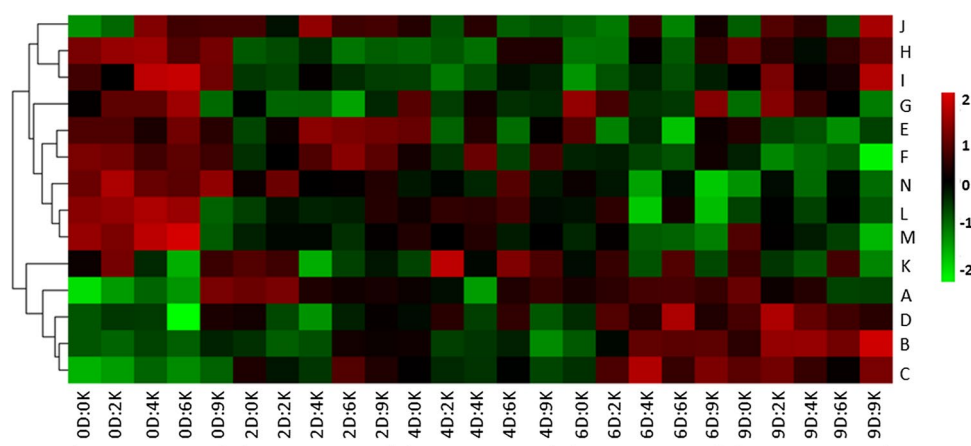


Fig. 3 Heatmap illustrating the occurrence of discriminatory ions in *M. oleifera* callus treated with different concentrations of PGRs (Table 1) and annotated as in Table 2. (A): Caffeoyl hexose; (B): Caffeoyl dihexose; (C): Coumaroyl aspartate; (D): Coumaroyl hexose; (E): Protocatechuic acid hexose; (F): Benzyl alcohol hexose pentose

isomer I; (G): Benzyl alcohol hexose pentose isomer II; (H): Phenylalanine; (I): Tryptophan; (J): Tryptophan conjugate; (K): Butanoyl hexose pentose; (L): Trihydroxyoctadecenoic acid isomer II; (M): Trihydroxyoctadecadienoic acid isomer II; (N): Trihydroxyoctadecadienoic acid isomer IV

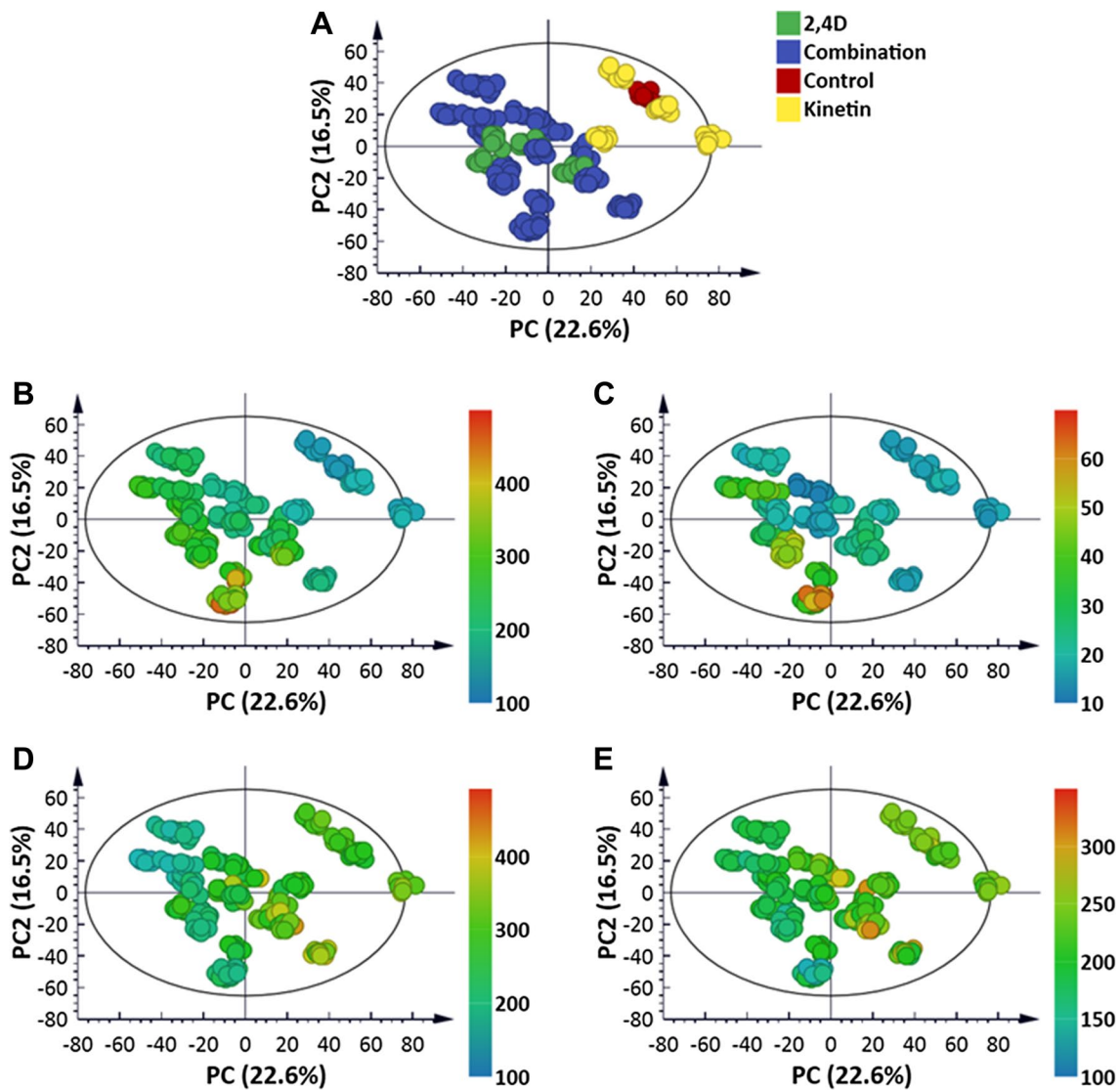


Fig. 4 Colour-coded PCA score plots showing the occurrence of selected compounds among *M. oleifera* callus treated with different concentrations of PGRs (Table 1) and analyzed by UHPLC–MS in

ESI negative mode. **a** All treatment coloured according to the group, **b** coumaroyl aspartate, **c** caffeoyl dihexose, **d** protocatechuic acid hexose and **e** benzyl alcohol isomer III

to these phytohormones and the interaction and/or the combination of some or all of these factors (Kevers et al. 1996; Leljak-Levanić et al. 2016).

In general, plant tissue differentiation is determined by the auxin-cytokinin ratio present in the media (Förster et al. 2013). The absence of organogenesis in the presence of either PGR alone (Figs. S2a, b respectively), and in combination (Fig. S2c), suggests that the *M. oleifera* callus cell line developed in this study had lost its totipotency, probably due to the habituation phenomenon. The reasons for the loss of regenerative ability of plant cells are also not well established. Nonetheless, three theories can be proposed to explain this phenomenon. The first is the genetic variation present in the original cell population (Gaspar et al. 2000).

The second theory is that during in vitro culture, substances promoting organogenesis may gradually diminish in the medium or a regeneration inhibitor may accumulate with time, leading to the suppression of organogenesis. The last theory is the occurrence of an epigenetic variation in the cultured cells (Kaepler et al. 2000). This is manifested as changes in the manner that gene expression occurs in the cultured cells caused by the environment of culture. An example of such variation is the in vitro hypo- or hypermethylation of genes involved in organogenesis, resulting in the modification of gene expression. Moreover, the change in metabolism, receptivity or transduction pathways of endogenous hormones may induce loss of totipotency (Lambé et al. 1997; Gaspar et al. 2000).

Similarly to this study, Shahzad et al. (2014) employed different PGRs: BAP (benzylaminopurine), Kin and NAA (1-naphthaleneacetic acid), alone and in combination, to induce regeneration of *M. oleifera* callus and did not observe organogenesis. However, in a study conducted by Mathur et al. (2014) maximum shoot regeneration of *M. oleifera* callus was observed on media enriched with BAP and Kin (BAP:Kin; 8:9 μM). Maximum root regeneration was observed on media supplemented with indole-3-butyric acid (IBA) and NAA (IBA:NAA; 10:2 μM). This implies that *M. oleifera* callus regeneration depends on many factors, including the type and ratio of PGRs employed, and also the state of the cells (habituated/non-habituated).

Total phenolics and anti-oxidant content

The total phenolic compound content assay reflects the reducing capacity of the extracts, and is also used as a general indicator of secondary metabolite synthesis in plants (Stojakowska et al. 2016). Variation was observed in the TPC following PGR treatment of *M. oleifera* calli (Table 1, Fig. S3), indicating that the production of phenolics was differentially affected by the concentration or ratio of PGRs present in the media. These observations confirm the interaction existing between auxins and cytokinins (Moubayidin et al. 2009). Plant growth regulators, especially auxins and/or cytokinins have been reported to modify the shikimate/phenylpropanoid pathway responsible for the biosynthesis of the phenolic acids (Moyo et al. 2014).

The phenolic content of the cultured cells did not correlate with the determined anti-oxidant activity. This suggests that the different PGR combinations and ratios have a differential effect on the secondary metabolite composition of the cultured callus. More precisely, this might imply that the anti-oxidant activity of *M. oleifera* callus is not only due to the presence and concentrations of phenolic compounds. Although the chemical composition and structures of phenolics present in extracts are important factors contributing to anti-oxidant activity, compounds such as ascorbic acid, carotenoids, sterols, aromatic amino acids and proteins also contribute (Choe and Min 2015). This highlights the complexity of anti-oxidative properties of plant extracts which can manifest in various ways (Nimse and Pal 2015). As seen in the current study, the composition of phenolic compounds in the extracts cannot easily be correlated to the anti-oxidant capacity thereof.

The effect of the different ratios of the two PGRs were also discernible in the UHPLC–MS chromatograms that depicted presence/absence of certain peaks as well as quantitative differences (Fig. 1). PCA in combination with HCA generated a visual presentation of the different metabolomes associated with the 25 conditions (Fig. 2) while OPLS-DA modelling allowed for the extraction of specific ions that

contributed to the variability between the various conditions (Figs. S4, S5).

Significance of the biomarker metabolites

The last step in a metabolomic study, namely metabolite annotation/identification, is a crucial for the biochemical interpretation of the data (Table 2). In *M. oleifera*, a large variety of metabolites has been identified in leaves, flowers and seeds (Rodríguez-Pérez et al. 2015; Ramabulana et al. 2016; Vats and Gupta 2017; Hamany Djande et al. 2018). The compounds include phenolics and flavonoids (Makita et al. 2016; Nouman et al. 2016; Hamany Djande et al. 2018), glucosinolates (glucomoringin) (Ramabulana et al. 2017), terpenes and alkaloids (Saini et al. 2016).

With the development of analytical platforms such as UHPLC–ESI–MS for secondary metabolite analyses, LC–MS has become a method of choice for metabolomic approaches, especially non-targeted metabolomics (Mareya et al. 2019). Although several studies have been reported for *M. oleifera* leaves, these have not been extended to profiling the phytochemicals present in undifferentiated callus cultures.

Hydroxycinnamic acid derivatives are widely distributed phytochemicals and constitute the main class of the phenylpropanoid metabolites found in nature (Macoy et al. 2015). Caffeoyl-hexose has been reported in *Nicotiana tabacum* cell suspensions (Mudau et al. 2018) and coumaroyl aspartate in cacao beans (Pereira-Caro et al. 2013), *Arabidopsis thaliana* (Mock et al. 1993) and *Solanum tuberosum* cell suspension cultures (Keller et al. 1996). Coumaroyl hexose has been detected in the pulp and seed extracts of *Melicoccus bijugatus* (Bystrom et al. 2011). HCA are well-known as inhibitors of lipid peroxidation and radical scavengers, and play a role in plant defense against insects and pathogens (Stojakowska et al. 2016).

The hydroxybenzoic acid has been reported in many plants (Fang et al. 2007; Khoddami et al. 2013; Mudau et al. 2018). Protocatechuic acid is linked to plant defenses and known to display anti-microbial (Semaming et al. 2015), anti-apoptotic, anti-oxidant (Liu et al. 2008) and anti-fungal (Khadem and Marles 2010) activities. Benzyl alcohols are benzoic acid precursors or intermediates for the synthesis of essential molecules (Widhalm and Dudareva 2015) and have similarly been reported in several plants (Bystrom et al. 2011; Hurtado-Fernández et al. 2011; Barros et al. 2012; Mudau et al. 2018). These are volatile organic compounds playing a role in defenses of *Solanum* species, e.g. exhibiting anti-microbial activities (Widhalm and Dudareva 2015).

Primary metabolites such as aromatic amino acids Phe and Trp are essential compounds in plant metabolism, and play a role as precursors for many secondary metabolites involved in adaptive plant stress responses. While it is

possible that the aromatic amino acids might have played a role in the determined DPPH scavenging activity, the reprogrammed cellular metabolome could have also contributed to the antioxidant properties observed.

Metabolite profiles of differentiated and undifferentiated tissue of *M. oleifera*

In our recent study (Hamany Djande et al. 2018), using the same UHPLC–MS analytical platform as described, extracts from *M. oleifera* leaf tissue were found to contain glucosinolates (glucomoringin), phenolics and phenolic conjugates such as chlorogenic acid and CGA derivatives; and flavonoids (quercetin, kaempferol, isorhamnetin and apigenin attached to one or more sugar moieties). Surprisingly, glucosinolates, CGAs and flavonoids were all not detected in the callus initiated from *M. oleifera* stem sections. Metabolites associated with the early steps of the diverging phenylpropanoid pathway were, however, detected e.g. derivatives of benzoic acids and cinnamic acids and cinnamic acids conjugated to either one or two sugars moieties. Interestingly, coumaroyl aspartate and protocatechuic acid hexose were identified in callus, and have not been reported in *M. oleifera* leaves thus far (Rodríguez-Pérez et al. 2015; Hamany Djande et al. 2018). This shows that for secondary metabolite production, *M. oleifera* differentiated leaf tissue and undifferentiated callus share similar pathways, but that the sub-pathways leading to CGAs and flavonoids were repressed in callus, thus leading to dramatically different metabolite profiles.

The shikimate/chorismate pathway leads to the production of secondary metabolites, and it is clear that enzymes involved to the formation of the amino acids Trp and Phe (precursors of secondary metabolites) are active in both differentiated leaf tissue and undifferentiated callus. The production of coumaroyl glycoside and caffeoyl hexose can either occur through the formation of coumaric acid and caffeic acid respectively [involving enzymes such as cinnamate 4-hydroxylase (C4H)], or the conversion of trans-cinnamic acid to cinnamoyl glucose (involving cinnamate glucosyl transferase). Coumaroyl aspartate, on the other hand, results from the conjugation of coumaric acid and aspartic acid. The pathway leading to the formation of CGAs and flavonoids, via the conversion of coumaric acid to coumaroyl-CoA with the enzyme 4-coumarate-CoA ligase (4CL), seems to be repressed in undifferentiated callus tissue as none of these metabolites was found in this *M. oleifera* callus line. In addition, the committing gene responsible of the biosynthesis of Phe-derived glucosinolates (the cytochrome P450, *CYP79A2*) in leaves is most likely inactivated in callus

cultures, resulting in the absence of glucomoringin (Fig. 5) (Tzin and Galili 2010; Morreel et al. 2014; Widhalm and Dudareva 2015).

There are limited reports comparing the metabolite profiles of differentiated tissue versus undifferentiated callus cultures. However, related studies on undifferentiated cell suspension cultures have found similar results. For instance, non-habituated *Nicotiana tabacum* (Ncube et al. 2014) and *Centella asiatica* (Ncube et al. 2016) cell suspensions exhibited different secondary metabolite distribution profiles compared to differentiated leaf tissue and hairy root cultures of intact beetroot plants exhibited differences in metabolite production (Georgiev et al. 2010). Although the habituation phenomenon can be responsible for the differential metabolite profiling observed in *M. oleifera* callus, the evidence behind this assumption is not established. On the contrary, it was demonstrated in *Catharanthus roseus* that habituated cells produce higher amounts of alkaloids in comparison to non-habituated cells (Merillon et al. 1989).

Conclusion

This work aimed to investigate the effects of auxin (2,4-D) and cytokinin (Kin) on the ability of undifferentiated *M. oleifera* callus cells to regenerate; and to screen and study the metabolite distribution resulting from the alterations in concentrations and combinations of the PGRs. However, following treatment with different 2,4-D/Kin ratios to initiate organogenesis, no redifferentiation of roots or shoots was observed. This was probably due to the observed habituation phenomenon. Nevertheless, metabolomic profiling of callus extracts revealed that the habituated cells did retain the ability to respond to external growth regulator manipulation, as reflected in differential levels of total phenolics and anti-oxidant compounds. Strikingly, the total absence of CGAs, flavonoids and glucosinolates were observed, against a background of differential accumulation of phenolic compounds and anti-oxidants that included derivatives of hydroxycinnamic acids and hydroxybenzoic acids. In addition to the regulatory/inhibitory effects of the PGRs on the production of secondary metabolites, the effect of the auxin: cytokinin ratios on the metabolite profiles were also apparent. The phytochemical diversity and complexity of *M. oleifera* systems could also be attributed to the genetic variation therein, and the suppression or activation of the gene expression encoding enzymes involved in the biosynthesis of the secondary metabolites.

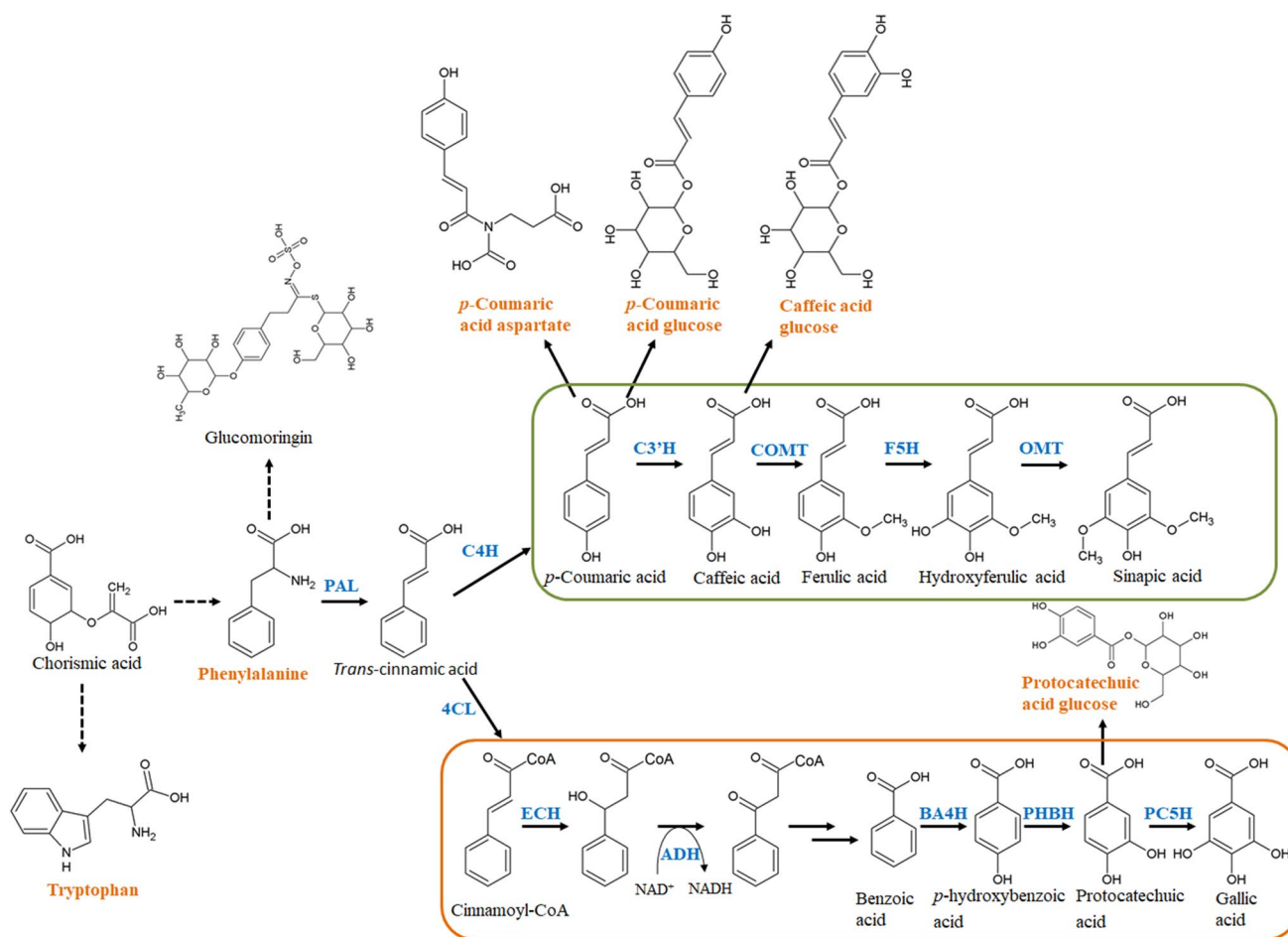


Fig. 5 Possible routes taken by *M. oleifera* for the production of secondary metabolites identified in callus tissue exposed to differing concentrations and ratios of 2,4-D and Kin. The pathway initiates with the formation of chorismic acid from the shikimate pathway. Dashed arrows designate multiple reactions before the formation of a class of compounds. Names of selected biomarkers identified in the study are in bold. The upper box represents the pathway leading to the formation of hydroxycinnamic acids and the lower one shows the

reactions leading to hydroxybenzoic acids. Enzymes involved are: *PAL* phenylalanine ammonia-lyase, *C4H* cinnamoyl hydroxylase, *C3'H* *p*-coumarate 3'-hydroxylase, *COMT* caffeic acid 3-*O*-methyltransferase, *F5H* ferulate 5-hydroxylase, *OMT* *O*-methyltransferase, *4CL* 4-hydroxycinnamoyl-CoA ligase, *ECH* enoyl-CoA hydratase, *ADH* cinnamoyl alcohol dehydrogenase, *BA4H* benzoic acid 4-hydroxylase, *PHBH* *p*-hydroxybenzoic acid 3-hydroxylase, *PC5H* protocatechuic acid 5-hydroxylase

Acknowledgements The South African National Research Foundation (NRF) is thanked for grant support to NEM (Grant No. 107067) and IAD (Grant No. 95818) and fellowship support to CHD.

Author Contributions IAD and NEM conceived and supervised the project. YHD performed the experimental work and PAS the instrumental analysis. CHD and NEM analysed the data. All authors contributed to writing and editing the manuscript. All authors have read and approved the final version of the manuscript.

Compliance with ethical standards

Conflict of interest The authors declare no conflict of interest.

References

- Ainsworth EA, Gillespie KM (2007) Estimation of total phenolic content and other oxidation substrates in plant tissues using Folin-Ciocalteu reagent. *Nat Protoc* 2:875–877
- Avila-Treviño JA, Muñoz-Alemán JM, Pérez-Molphe-Balch E, Rodríguez-Sahagún A, Morales-Domínguez JF (2017) In vitro propagation from bud and apex explants of *Moringa oleifera* and evaluation of the genetic stability with RAMP marker. *S Afr J Bot* 108:149–156
- Barros L, Dueñas M, Pinela J, Carvalho AM, Buelga CS, Ferreira ICF (2012) Characterization and quantification of phenolic compounds in four tomato (*Lycopersicon esculentum* L.) farmers' varieties in Northeastern Portugal homegardens. *Plant Foods Hum Nutr* 67:229–234
- Bystrom LM, Lewis BA, Brown DL, Rodriguez E, Obendorf RL (2011) Characterization of phenolics by LC–UV/vis, LC–MS/

- MS and sugars by GC in *Melicoccus bijugatus* Jacq. “Montgomery” fruits. *Food Chem* 111:1017–1024
- Choe E, Min DB (2015) Mechanisms of antioxidants in the oxidation of foods. *Compr Rev Food Sci Food Saf* 8:345–358
- Deshpande S, Matei MF, Jaiswal R, Bassil BS, Kortz U, Kuhnert N (2016) Synthesis, structure, and tandem mass spectrometric characterization of the diastereomers of quinic acid. *J Agric Food Chem* 64:7298–7306
- Esterhuizen L, Meyer R, Dubery I (2006) Antioxidant metabolites from *Coleonema album*. *Nat Prod Commun* 1:367–375
- Fang Z, Zhang M, Wang L (2007) HPLC-DAD-ESIMS analysis of phenolic compounds in bayberries (*Myrica rubra* Sieb. et Zucc.). *Food Chem* 100:845–852
- Förster N, Mewis I, Ulrichs C (2013) *Moringa oleifera*. Establishment and multiplication of different ecotypes in vitro. *Gesunde Pflanz* 65:21–31
- Fusani P, Piwowarski JP, Zidorn C, Kiss AK, Scartezzini F, Granica S (2016) Seasonal variation in secondary metabolites of edible shoots of Buck’s beard [*Aruncus dioicus* (Walter) Fernald (Rosaceae)]. *Food Chem* 202:23–30
- Gaspar T, Kevers C, Bisbis B, Franck T, Crevecoeur M, Greppin H, Dommes J (2000) In vitro plant recalcitrance loss of plant organogenic totipotency in the course of in vitro neoplastic progression. *In Vitro Cell Dev Biol Plant* 36:171–181
- George EF, Hall MA, Klerk GJ (2008) Plant growth regulators I: introduction; auxins, their analogues and inhibitors. In: George EF, Hall MA, Klerk GJ (eds) *Plant propagation by tissue culture*, vol 1. Springer, Dordrecht. pp 175–204
- Georgiev VG, Weber J, Kneschke EM, Denev PN, Bley T, Pavlov AI (2010) Antioxidant activity and phenolic content of betalain extracts from intact plants and hairy root cultures of the red beetroot *Beta vulgaris* cv. Detroit dark red. *Plant Foods Hum Nutr* (Dordrecht, the Netherlands) 65:105–111
- Gupta S, Jain R, Kachhwaha S, Kothari SL (2018) Nutritional and medicinal applications of *Moringa oleifera* Lam.—Review of current status and future possibilities. *J Herb Med* 11:1–11
- Hagege D (1996) Habituation in sugarbeet plant cells: Permanent stress or antioxidant adaptative strategy? *In Vitro Cell Dev Biol Plant* 32:1–5
- Hamany Djande CY, Piater LA, Steenkamp PA, Madala NE, Dubery IA (2018) Differential extraction of phytochemicals from the multipurpose tree, *Moringa oleifera*, using green extraction solvents. *S Afr J Bot* 115:81–89
- Hassanein AM, Salem JM, Faheed FA, El-nagishet A (2018) Effect of anti-ethylene compounds on isoenzyme patterns and genome stability during long term culture of *Moringa oleifera*. *Plant Cell Tissue Organ Cult* 132:201–212
- Hellwig S, Drossard J, Twyman RM, Fischer R (2004) Plant cell cultures for the production of recombinant proteins. *Nat Biotechnol* 22:1415–1422
- Hurtado-Fernández E, Pacchiarotta T, Gómez-Romero M, Schoenmaker B, Derks R, Deelder AM, Mayboroda OA, Carrasco-Pancorbo A, Fernández-Gutiérrez A (2011) Ultra-high performance liquid chromatography-time of flight mass spectrometry for analysis of avocado fruit metabolites: method evaluation and applicability to the analysis of ripening degrees. *J Chromatogr A* 1218:7723–7738
- Kaeppeler SM, Kaeppeler HF, Rhee Y (2000) Epigenetic aspects of somaclonal variation in plants. *Plant Mol Biol* 43:179–188
- Karar MGE, Kuhnert N (2015) UPLC-ESI-Q-TOF-MS/MS characterization of phenolics from *Crataegus monogyna* and *Crataegus laevigata* (hawthorn) leaves, fruits and their herbal derived drops (Crataegutt tropfen). *J Chem Biol Ther.* <https://doi.org/10.4172/2572-0406.1000102>
- Keller H, Hohlfeld H, Wray V, Hahlbrock K, Scheel D, Strack D (1996) Changes in the accumulation of soluble ad cell wallbound phenolics in elicitor-treated cell suspension cultures and fungus-infected leaves of *Solanum tuberosum*. *Phytochemistry* 42:2–9
- Kevers C, Filali M, PetitPaly G, Hagege D, Rideau M, Gaspar T (1996) Habituation of plant cells does not mean insensitivity to plant growth regulators. *In Vitro Cell Dev Biol Plant* 32:204–209
- Khadem S, Marles RJ (2010) Monocyclic phenolic acids; hydroxy- and polyhydroxybenzoic acids: occurrence and recent bioactivity studies. *Molecules* 15:7985–8005
- Khoddami A, Wilkes MA, Roberts TH (2013) Techniques for analysis of plant phenolic compounds. *Molecules* 18:2328–2375
- Kind T, Fiehn O (2007) Seven Golden Rules for heuristic filtering of molecular formulas obtained by accurate mass spectrometry. *BMC Bioinformatics* 8:1–20. <https://doi.org/10.1186/1471-2105-8-105>
- Lambé P, Mutambel HSN, Fouché JG, Deltour R, Foidart JM, Gaspar T (1997) DNA methylation as a key process in regulation of organogenic totipotency and plant neoplastic progression? *In Vitro Cell Dev Biol Plant* 33:155–162
- Leljak-Levanić D, Mrvková M, Turečková V, Pěnčík A, Rolčík J, Strnad M, Mihaljević S (2016) Hormonal and epigenetic regulation during embryogenic tissue habituation in *Cucurbita pepo* L. *Plant Cell Rep* 35:77–89
- Liu Y, Jiang B, Bao Y, An L (2008) Protocatechuic acid inhibits apoptosis by mitochondrial dysfunction in rotenone-induced PC12 cells. *Toxicol in Vitro* 22:430–437
- Loyola-Vargas VM, Ochoa-Alejo N (2012) An introduction to plant cell culture: the future ahead. In: Loyola-Vargas VM, Ochoa-Alejo N (eds) *Plant cell culture protocols*, 3rd edn. Springer, New York, pp 1–8. <https://doi.org/10.1007/978-1-61779-818-4>
- Macoy DM, Kim WY, Lee SY, Kim MG (2015) Biotic stress related functions of hydroxycinnamic acid amide in plants. *J Plant Biol* 58:156–163
- Makita C, Chimuka L, Steenkamp P, Cukrowska E, Madala E (2016) Comparative analyses of flavonoid content in *Moringa oleifera* and *Moringa ovalifolia* with the aid of UHPLC-qTOF-MS fingerprinting. *S Afr J Bot* 105:116–122
- Mareya C, Tugizimana F, Piater L, Madala NE, Steenkamp PA, Dubery IA (2019) Untargeted metabolomics reveal defense-related metabolic reprogramming in *Sorghum bicolor* against infection by *Burkholderia andropogonis*. *Metabolites* 9:8. <https://doi.org/10.3390/metabo9010008>
- Mathur M, Yadav S, Katariya PK, Kamal R (2014) In vitro propagation and biosynthesis of steroidal sapogenins from various morphogenetic stages of *Moringa oleifera* Lam., and their antioxidant potential. *Acta Physiol Plant* 36:1749–1762. <https://doi.org/10.1007/s11738-014-1549-1>
- Merillon J, Quelhazii L, Doireau P, Chenieux J, Rideau M (1989) Metabolic changes and alkaloid production in habituated and non-habituated cells of *Catharanthus roseus* grown in hormone-free medium. Comparing hormone-deprived non-habituated cells with habituated cells. *J Plant Physiol* 134:54–60
- Mock H-P, Wray V, Beck W, Metzger JW, Strack D (1993) Coumaroylaspartate from cell suspension cultures of *Arabidopsis thaliana*. *Phytochemistry* 1:157–159
- Morreel K, Saeys Y, Dima O, Lu F, Van de Peer Y, Vanholme R, Ralph J, Vanholme B, Boerjan W (2014) Systematic structural characterization of metabolites in *Arabidopsis* via candidate substrate-product pair networks. *Plant Cell* 26:929–945
- Moubayidin L, Di Mambro R, Sabatini S (2009) Cytokinin–auxin crosstalk. *Trends Plant Sci* 14:557–562
- Moyo M, Amoo SO, Aremu AO, Gruz J, Šubrtová M, Doležal K, Van Staden J (2014) Plant regeneration and biochemical accumulation of hydroxybenzoic and hydroxycinnamic acid derivatives

- in *Hypoxis hemerocallidea* organ and callus cultures. *Plant Sci* 227:157–164
- Mudau SP, Steenkamp PA, Piater LA, De Palma M, Tucci M, Madala NE, Dubery IA (2018) Metabolomics-guided investigations of unintended effects of the expression of the hydroxycinnamoyl quinate hydroxycinnamoyltransferase (*hqt1*) gene from *Cynara cardunculus* var. *scolymus* in *Nicotiana tabacum* cell cultures. *Plant Physiol Biochem* 127:287–298
- Mughal MHS, Ali G, Srivastava PS, Iqbal M (1999) Improvement of drumstick (*Moringa pterygosperma* Gaertn.)—A unique source of food and medicine through tissue culture. *Hamdard Med* 42:37–42
- Murashige T, Skoog F (1962) A revised medium for rapid growth and bio assays with tobacco tissue cultures. *Physiol Plant* 15:473–497
- Ncube E, Mhlongo M, Piater L, Steenkamp P, Dubery IA, Madala N (2014) Analyses of chlorogenic acids and related cinnamic acid derivatives from *Nicotiana tabacum* tissues with the aid of UPLC-qTOF-MS/MS based on the in-source collision-induced dissociation method. *Chem Cent J* 8:1–10
- Ncube EN, Steenkamp PA, Madala NE, Dubery IA (2016) Chlorogenic acids biosynthesis in *Centella asiatica* cells is not responsive to salicylic acid manipulation. *Appl Biochem Biotechnol* 179:685–696
- Nimse SB, Pal D (2015) Free radicals, natural antioxidants, and their reaction mechanisms. *RSC Adv* 5:27986–28006
- Nouman W, Anwar F, Gull T, Newton A, Rosa E, Domínguez-Perles R (2016) Profiling of polyphenolics, nutrients and antioxidant potential of germplasm's leaves from seven cultivars of *Moringa oleifera* Lam. *Ind Crops Prod* 83:166–176
- Ochoa-Villarreal M, Howat S, Jang MO, Kim IS, Jin Y, Lee E, Loake GJ (2015) Cambial meristematic cells: a platform for the production of plant natural products. *New Biotechnol* 32:581–587
- Ochoa-Villarreal M, Howat S, Hong S, Jang MO, Jin Y, Lee E, Loake GJ (2016) Plant cell culture strategies for the production of natural products. *Biochem Mol Biol Rep* 49:149–158
- Pereira-Caro G, Borges G, Nagai C, Jackson MC, Yokota T, Crozier A, Ashihara H (2013) Profiles of phenolic compounds and purine alkaloids during the development of seeds of *Theobroma cacao* cv. Trinitario. *J Agric Food Chem* 61:427–434
- Radić S, Vujčić V, Glogoški M, Radić-Stojković M (2016) Influence of pH and plant growth regulators on secondary metabolite production and antioxidant activity of *Stevia rebaudiana* (Bert). *Period Biol* 118:9–19
- Ramabulana T, Mavunda RD, Steenkamp PA, Piater LA, Dubery IA, Madala NE (2016) Perturbation of pharmacologically relevant polyphenolic compounds in *Moringa oleifera* against photo-oxidative damages imposed by gamma radiation. *J Photochem Photobiol B* 156:79–86
- Ramabulana T, Mavunda RD, Steenkamp PA, Piater LA, Dubery IA, Ndhala AR, Madala NE (2017) Gamma radiation treatment activates glucomoringin synthesis in *Moringa oleifera*. *Rev Bras Farmacogn* 27:569–575
- Rodríguez-Pérez C, Quirantes-Piné R, Fernández-Gutiérrez A, Segura-Carretero A (2015) Optimization of extraction method to obtain a phenolic compounds-rich extract from *Moringa oleifera* Lam leaves. *Ind Crops Prod* 66:246–254
- Saini RK, Sivanesan I, Keum Y (2016) Phytochemicals of *Moringa oleifera*: a review of their nutritional, therapeutic and industrial significance. *3 Biotech* 6:203
- Salem JM (2016) In vitro propagation of *Moringa oleifera* L. under salinity and ventilation conditions. *Genet Plant Physiol* 6:54–64
- Semaming Y, Pannengetch P, Chattipakorn SC, Chattipakorn N (2015) Pharmacological properties of protocatechuic acid and its potential roles as complementary medicine. *Evid Based Complement Altern Med*. <https://doi.org/10.1155/2015/593902>
- Shahzad U, Jaskani MJ, Ahmad S, Awan FS (2014) Optimization of the micro-cloning system of threatened *Moringa oleifera* Lam. *Pak J Agric Sci* 51:449–457
- Shank LP, Lee VS, Dheeranupattana S (2013) Peroxidase activity in native and callus culture of *Moringa oleifera* Lam. *J Med Bioeng* 2:163–167
- Sriskandarajah S, Prinsen E, Motyka V, Dobrev PI, Serek M (2006) Regenerative capacity of cacti *Schlumbergera* and *Rhipsalidopsis* in relation to endogenous phytohormones, cytokinin oxidase/dehydrogenase, and peroxidase activities. *J Plant Growth Regul* 25:79–88
- Srivastava MNS (2017) Elicitation: a stimulation of stress in in vitro plant cell/tissue cultures for enhancement of secondary metabolite production. *Phytochem Rev* 16:1227–1252
- Stojakowska A, Malarz J, Kiss AK (2016) Hydroxycinnamates from elecampane (*Inula helenium* L.) callus culture. *Acta Physiol Plant* 38:41
- Sumner LW, Amberg A, Barrett D, Beale MH, Beger R, Daykin CA et al (2007) Proposed minimum reporting standards for chemical analysis: Chemical Analysis Working Group (CAWG) Metabolomics standards initiative. *Metabolomics* 3:211–221
- Tiloke C, Anand K, Gengan RM, Chuturgoon AA (2018) *Moringa oleifera* and their phytonanoparticles: Potential antiproliferative agents against cancer. *Biomed Pharmacother* 108:457–466
- Tugizimana F, Dubery I, Piater L (2013) Plant metabolomics: a new frontier in phytochemical analysis. *S Afr J Sci* 109(5/6):1–11
- Tugizimana F, Steenkamp P, Piater L, Dubery I (2016) A conversation on data mining strategies in LC-MS untargeted metabolomics: pre-processing and pre-treatment steps. *Metabolites* 6:40
- Tzin V, Galili G (2010) The biosynthetic pathways for shikimate and aromatic amino acids in *Arabidopsis thaliana*. *Arabidopsis B* 8:e0132
- Vats S, Gupta T (2017) Evaluation of bioactive compounds and antioxidant potential of hydroethanolic extract of *Moringa oleifera* Lam. from Rajasthan, India. *Physiol Mol Biol Plants* 23:239–248
- Widhalm JR, Dudareva N (2015) A familiar ring to it: biosynthesis of plant benzoic acids. *Mol Plant* 8:83–97

Publisher's Note Springer Nature remains neutral with regard to jurisdictional claims in published maps and institutional affiliations.